Tensile drawing behaviour of a linear low-density polyethylene: Changes in physical and mechanical properties

R. Seguela and F. Rietsch
Laboratoire de Structure et Propriétés de l'Etat Solide, LA 234, Université des Sciences et Techniques de Lille, 59655, Villeneuve d'Ascq, France
(Received 19 February 1985)

The tensile drawing behaviour at 80°C of a linear low-density polyethylene has been investigated with particular attention to the changes in crystallinity, molecular orientation and mechanical properties. It was found that the more defective crystals were destroyed during drawing and rebuilt into more perfect crystals. Moreover, the crystallinity was improved by the strain-induced crystallization of initially amorphous chains. The crystalline chains quickly reached a nearly perfect orientation upon drawing, while the amorphous chains exhibited a slow and poor orientation. This contrasted with the spectacular increase in the tensile modulus of the fibres. It was suggested that the fibre stiffness is more sensitive to the number of intercrystalline tie molecules than to the chain tautness. On the other hand, the increase in tensile strength with draw ratio gave evidence that hot drawing is more efficient in generating intercrystalline tie molecules than cold drawing.

(Keywords: linear low-density polyethylene; hot drawing; crystallinity; molecular orientation; stiffness; strength)

INTRODUCTION

Owing to improvements in ethylene polymerization techniques, copolymers of ethylene with α-olefins have seen increasing development in the last ten years. The main technological interest in the so-called linear low-density polyethylenes (LLDPE) lies in their mechanical and thermal properties, which surpass those of conventional branched low-density polyethylenes. But, till now, very few studies[1-3] have been published about these novel materials.

LLDPE may be very useful from a theoretical standpoint to help in understanding the role played by amorphous chains in the drawing process of semicrystalline polymers. Indeed, the amount of elastomeric amorphous phase in LLDPE can vary over a wide range depending on the comonomer content, thus providing a direct way of tackling the problem of the specific behaviour of the amorphous chains.

In our previous work[2] we studied the effects of drawing conditions on the drawability of LLDPE. The stress–strain curves were quite different from those usually observed for high-density polyethylene (HDPE) and exhibited a marked strain-hardening effect. This was ascribed to an unfavourable molecular configuration of the amorphous phase, which hindered chain unfolding and microfibril slipping processes.

The goal of the present paper was to investigate the changes in crystallinity, thermal behaviour, molecular orientation and mechanical properties that occur during the tensile drawing of LLDPE. Correlations established between the various properties provide more information on the drawing mechanism.

EXPERIMENTAL

Material and preparation

The material studied is an ethylene–butene copolymer supplied by CdF Chimie. The number- and weight-average molecular weights are $M_n = 4.6 \times 10^4$ and $M_w = 1.6 \times 10^5$. The nominal density is 0.930 g cm^{-3}.

The polymer was compression moulded at 160°C and held for 10 min at this temperature before cooling at about 1°C min^{-1}. Sheets 1.7 mm and 0.4 mm thick were prepared, the latter being used for tensile strength measurements, together with birefringence measurements at low strains.

Drawing and mechanical testing

Dumbbell-shaped samples of gauge length 24 mm and width 5 mm were cut from the sheets and drawn at 80°C in an Instron Tensile Testing Machine operated at a cross-head speed of 50 mm min^{-1}. The tensile modulus of the fibres at room temperature was computed from the initial slope of the stress–strain curves recorded at a cross-head speed of 1 mm min^{-1}, using samples 80 mm long. The mechanical behaviour of the fibres up to rupture was determined at room temperature, using a cross-head speed of 50 mm min^{-1}, the sample length being 50 mm.

Crystallinity

Density determinations were performed in a water–isopropanol gradient column at 23°C. The volume crystallinity was estimated from the following equation:

$$\alpha_c^v = (\rho - \rho_a)/(\rho_c - \rho_a)$$

which assumes a perfect two-phase model, with the values $\rho_a = 0.855$ g cm^{-3} and $\rho_c = 1.000$ g cm^{-3} for the amorphous and crystalline densities, respectively[4-6].

Calorimetric investigations were carried out on a Perkin–Elmer DSC-2 apparatus at a heating rate of 10°C min^{-1}. The sample weight was about 7 mg. The volume crystallinity was calculated from the relation:

$$\alpha_c^v = (\rho/\rho_c) \times (\Delta H_f/\Delta H_f^*)$$

assuming $\Delta H_f^* = 69$ cal g^{-1} for the enthalpy of fusion of

0032-3861/86/040532-05$03.00

an infinite perfect crystal of polyethylene at $T_f = 140°C$.[6] The influences of crystal size, comonomer inclusion[7] and melting point depression[6] on the enthalpy of fusion ΔH_f of the actual crystal were neglected.

X-ray diffraction

The crystal orientation of the drawn samples was investigated on X-ray flat film patterns by scanning the (110) and (200) reflections with a Siemens microdensitometer. The crystalline orientation function:

$$f_c = \tfrac{3}{2}\langle\cos^2\phi\rangle_c - \tfrac{1}{2}$$

characterizing the polymer chain orientation in the crystalline phase was computed via the Wilchinsky relations[8]:

$$\langle\cos^2\phi\rangle_a = \langle\cos^2\phi\rangle_{200}$$
$$\langle\cos^2\phi\rangle_b = 1.445\langle\cos^2\phi\rangle_{110} - 0.445\langle\cos^2\phi\rangle_{200}$$

and taking into account that:

$$\langle\cos^2\phi\rangle_c = 1 - \langle\cos^2\phi\rangle_a - \langle\cos^2\phi\rangle_b$$

The crystalline lattice spacings d_{110} and d_{200} were estimated from the same X-ray patterns. The (002) line of β-graphite powder spread on the sample surface was used as reference, with a characteristic Bragg spacing $d_{002} = 3.405$ Å. The volume of the crystalline unit cell was calculated assuming a constant value of the lattice parameter $c = 2.55_0$ Å.[5,9]

Birefringence

A Leitz polarizing microscope equipped with an Ehringhaus compensator was used to measure the birefringence Δn_t of the fibres. The amorphous chain orientation f_a was estimated according to the relation:

$$\Delta n_t = f_c \Delta n_c^o \alpha_c^v + f_a \Delta n_a^o (1 - \alpha_c^v) + \Delta n_f$$

where the form birefringence Δn_f was neglected. The values of the crystalline and amorphous intrinsic birefringences used for the calculations were $\Delta n_c^o = 0.058$ and $\Delta n_a^o = 0.2$, respectively. The latter is an average value from several sources in the literature which argue in favour of a high optical anisotropy of the C–C bond[10-12].

RESULTS AND DISCUSSION

The first stage of plastic deformation of the present LLDPE is homogeneous up to draw ratio $\lambda \simeq 1.7$. On drawing beyond that strain, the well known fibrillar transformation takes place by yielding and neck formation, the characteristic draw ratio in the necked region being $\lambda^* \simeq 4$ when measured in the unloaded state. Neck propagation proceeds at roughly constant draw ratio over the full length of the sample, after which the deformation turns homogeneous again, up to rupture.

Crystallinity and thermal behaviour

Figure 1 shows the variation of volume crystallinity and melting point of the LLDPE as a function of draw ratio. Considering the assumptions and the oversimplified models involved in the calculation of crystallinity from

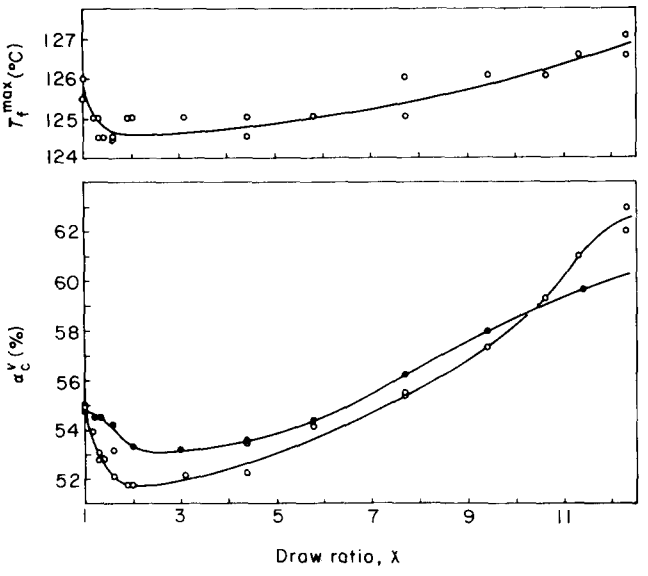

Figure 1 Volume crystallinity α_c^v and melting temperature T_f^{max} at the melting peak *versus* draw ratio for LLDPE drawn at 80°C: data from d.s.c. (○) and density (●)

density and melting enthalpy, the results of the two methods are in excellent agreement. The crystallinity decreases at first consequently to the shearing and the fragmentation of the crystalline lamellar ribbons in the spherulitic structure, before the fibrillar transformation. Then, during the necking process and the subsequent homogeneous drawing of the fibrillar structure, the crystallinity increases continuously, indicating a recrystallization of the chains pulled out of the crystals.

Peterlin *et al.*[13,14] reported a similar trend of variation for the crystallinity of HDPE as a function of draw ratio. However, for samples crystallized by slow cooling from the melt, the highest crystallinity reached by HDPE upon drawing is close to that in the isotropic state, while for LLDPE the crystallinity of the most drawn fibre greatly exceeds that of the starting material. Besides, in the case of LLDPE, the crystallinity obtained at the maximum draw ratio is very close to the crystallinity of a sample dried after crystallization from a dilute xylene solution, and subsequently annealed for four days at 115°C under slight pressure. This gives a clear indication that the drawing of LLDPE generates a strain-induced crystallization of some originally uncrystallized chains. These chains can be viewed as crystallizable sequences of ethylene units retained in the amorphous phase in the form of loose loops or intercrystalline tie molecules. Such situations related to the occurrence of non-adjacent re-entry foldings are sketched in *Figure 2*, according to the crystallization mechanism of random copolymers, which involves the exclusion of most of the comonomer units outside the crystalline phase (see the discussions in refs. 2 and 4). However, a small fraction of the comonomer units is trapped within the crystals as point defects (see ref. 9 and references cited therein), and it must be emphasized that the strain-induced crystallization is liable to enlarge this phenomenon by forced insertion of some isolated comonomer units.

It can be seen in *Figure 1* that the melting temperature T_m^{max} is not very sensitive to drawing. The slight increase observed beyond $\lambda = 2$ reveals that the lamellar crystalline blocks thicken on drawing, but not enough for the build-up of crystalline bridges[2], in contrast to HDPE[15].

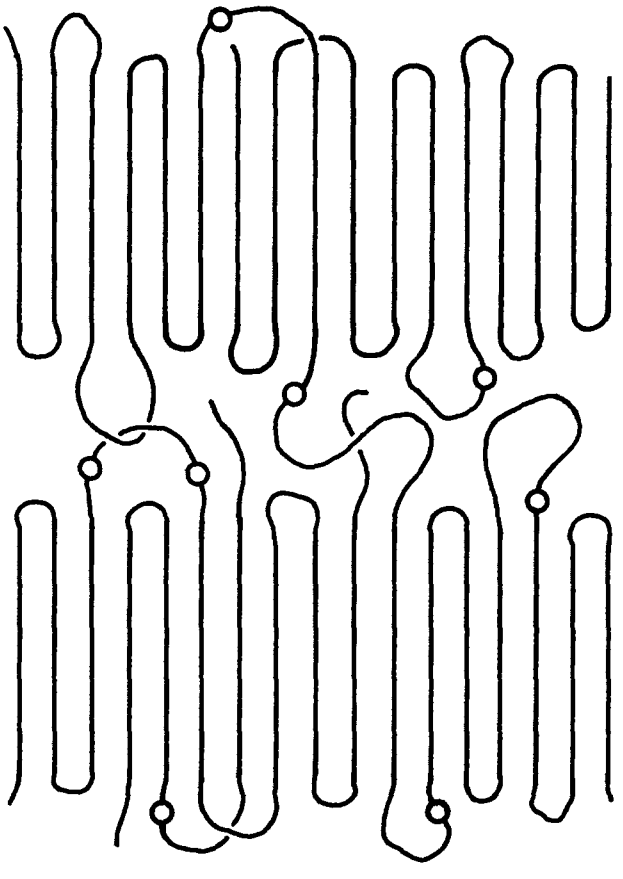

Figure 2 Two-phase model for LLDPE showing crystallizable chains retained in the intercrystalline amorphous layer; the open circles represent comonomer units (see text for details)

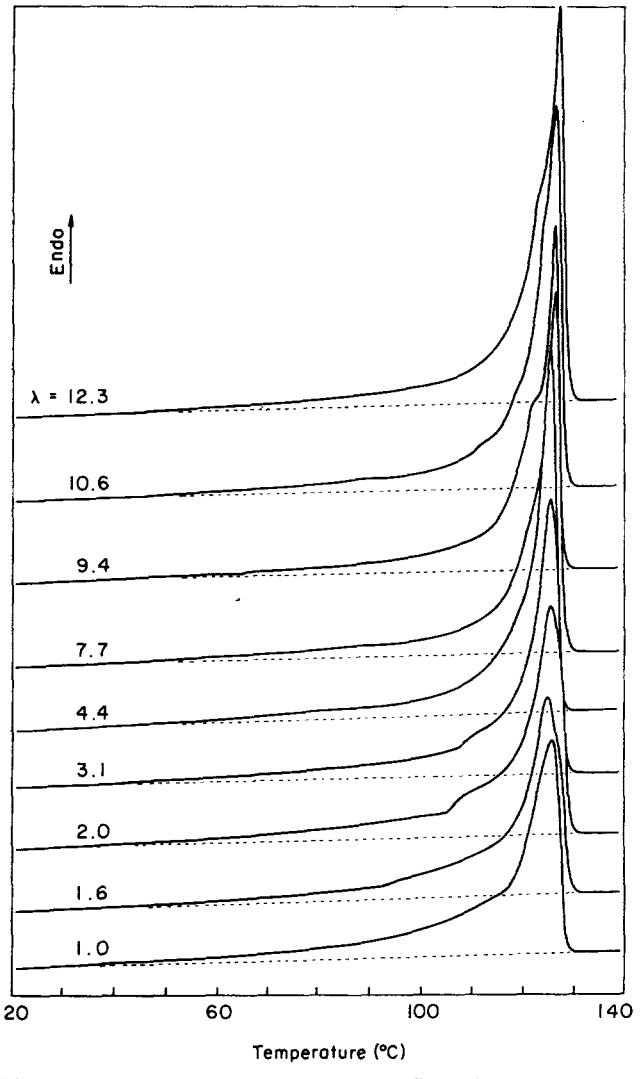

Figure 3 D.s.c. melting curves for LLDPE fibres drawn at 80°C for various draw ratios

The d.s.c. curves of *Figure 3* display the thermal behaviour of the LLDPE as a function of draw ratio. The gradual reduction in magnitude of the low-temperature melting tail, for draw ratio values up to $\lambda = 2$, indicates that the decrease in crystallinity already observed in *Figure 1* arises partly from the destruction of some of the less perfect crystals, these being the more mechanically compliant ones. Moreover, fragmentation of the large crystalline lamellae at the onset of the fibrillar transformation may also contribute to the lowering of crystallinity[13].

On drawing beyond the fibrillar transformation, i.e. for $\lambda > 4$, the main melting peak enhances and sharpens (*Figure 3*). This means that strain-induced crystallization narrows the crystal size distribution at the expense of the most defective crystals.

Unit cell volume

Measurements of the crystalline lattice parameters of LLDPE have been carried out in order to gain information about the development of the crystalline defects upon drawing. The variation of the unit cell volume is shown in *Figure 4* as a function of draw ratio. The crystalline unit cell of LLDPE prior to deformation is larger than that of HDPE, indicating inclusion of a few comonomer units within the crystalline lattice[9].

At the onset of drawing, the slight increase in the unit cell volume observed in *Figure 4* shows the nucleation of the crystalline defects required for the promotion of plastic deformation. Then, a decrease in unit cell volume occurs for $1.2 < \lambda < 2$, which can be associated with the

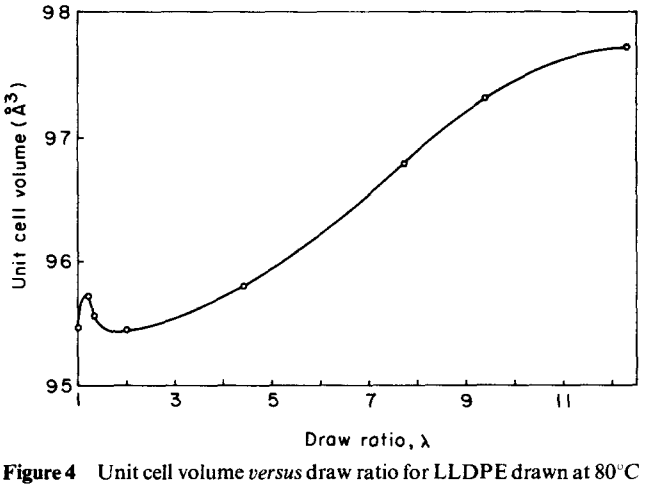

Figure 4 Unit cell volume *versus* draw ratio for LLDPE drawn at 80°C

destruction of the less perfect crystals containing the majority of the crystallized comonomer units. This has been previously concluded from the d.s.c. analysis. It is worth noting that Davis *et al.*[5] and Hosemann *et al.*[16,17] observed a similar decrease in the unit cell volume in plastically deformed linear and branched polyethylenes, respectively, but these authors gave quite different interpretations. The first authors suspected that the

phenomenon could result from a change in chain folding direction with deformation, while the second ones suggested that drawing promotes the migration of chain defects out of the lattice to optimize the crystallization. Our own interpretation is, however, supported by the change in crystallinity and the thermal behaviour.

For draw ratios $\lambda > 2$, the unit cell volume exhibits a steady increase that can be explained by an increase in paracrystalline disorder of the crystalline lattice, as proposed by Glenz *et al.*[18], who reported a similar expansion of the unit cell for HDPE drawn beyond necking. However, the unit cell expansion in LLDPE is much more pronounced than in HDPE. So, besides the paracrystalline disorder, we suspect that some comonomer units are incorporated by force into the crystal lattice as a result of the strain-induced crystallization of amorphous chains, as suggested above. It is to be noted that, during achievement of high drawing, the pulling of chains through crystalline blocks is liable to produce the same effect.

Molecular orientation

Figure 5 depicts the variations of the total birefringence together with the crystalline and non-crystalline birefringence contributions for the LLDPE, as a function of draw ratio. At the very beginning of drawing, the crystalline contribution exceeds the total birefringence, thus revealing a negative non-crystalline contribution. Branched low-density and linear high-density polyethylenes[19] and polypropylene[20] have previously been reported to give rise to a negative non-crystalline birefringence at low strain, which has been ascribed to an orientation of the amorphous chains perpendicular to the drawing direction. However, Kawai *et al.*[21,22] suggested more recently that the form birefringence in polyethylene could contribute negatively to the total birefringence at low strain, owing to the orientation of the crystalline lamellae associated with the detwisting of the lamellar ribbons in the equatorial zone of the spherulites.

For $\lambda > 1.4$, the non-crystalline birefringence becomes positive, as would be expected from the orientation of the amorphous chains in the drawing direction. This non-crystalline contribution tends to level off while the crystalline one exhibits a continuous rise with increase in crystallinity (see *Figure 1*).

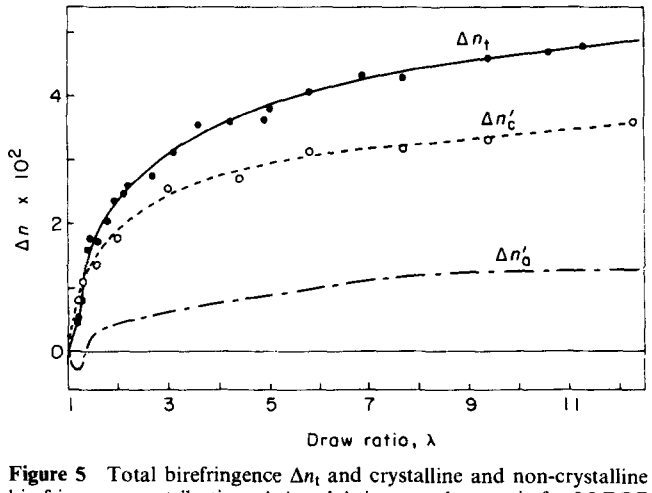

Figure 5 Total birefringence Δn_t and crystalline and non-crystalline birefringence contributions $\Delta n'_c$ and $\Delta n'_a$ *versus* draw ratio for LLDPE drawn at 80°C

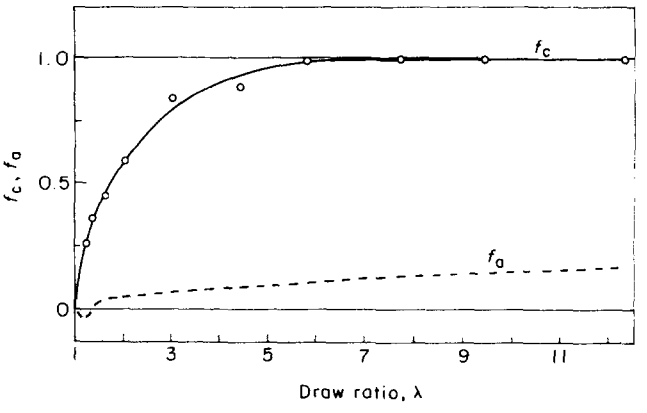

Figure 6 Crystalline and non-crystalline orientation functions f_c and f_a *versus* draw ratio for LLDPE drawn at 80°C

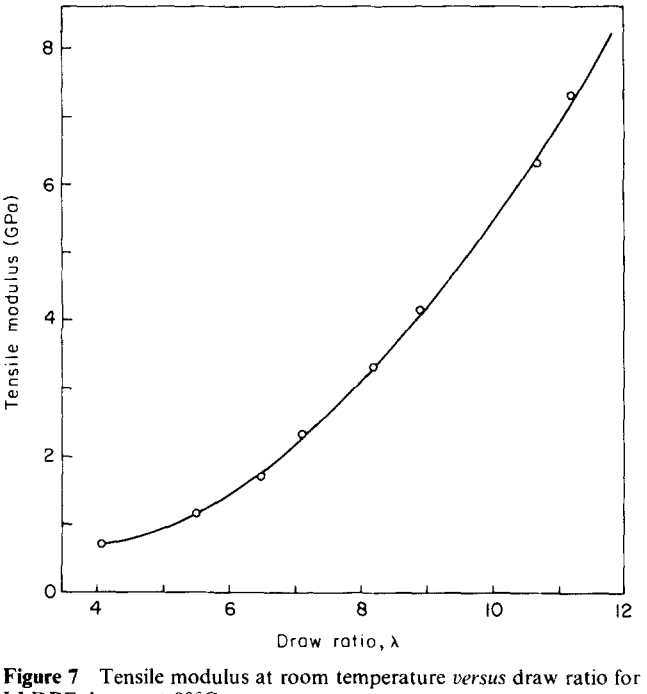

Figure 7 Tensile modulus at room temperature *versus* draw ratio for LLDPE drawn at 80°C

The variations of the crystalline and amorphous chain orientation functions are represented in *Figure 6*, assuming that the non-crystalline birefringence results from the amorphous chain orientation only. The crystalline phase quickly reaches a nearly perfect orientation while the amorphous phase orientates itself much more slowly and weakly. This latter result suggests relaxation of the elastomeric amorphous chains in the unloaded fibres, which is in agreement with the lack of crystalline bridges between the lamellar blocks along the fibre axis previously deduced from the d.s.c. analysis.

Mechanical properties

The variation of the tensile modulus *versus* draw ratio of the LLDPE is shown in *Figure 7*. This curve roughly follows the relationship previously reported by a number of authors for the drawing of melt-crystallized HDPE[13,23-25]. Nevertheless, owing to a much reduced drawability, LLDPE exhibits a maximum value of the tensile modulus about 10 times lower than for HDPE. Such a divergence is much more important than could be expected from the difference in crystal content only and should rather be related to structural and topological

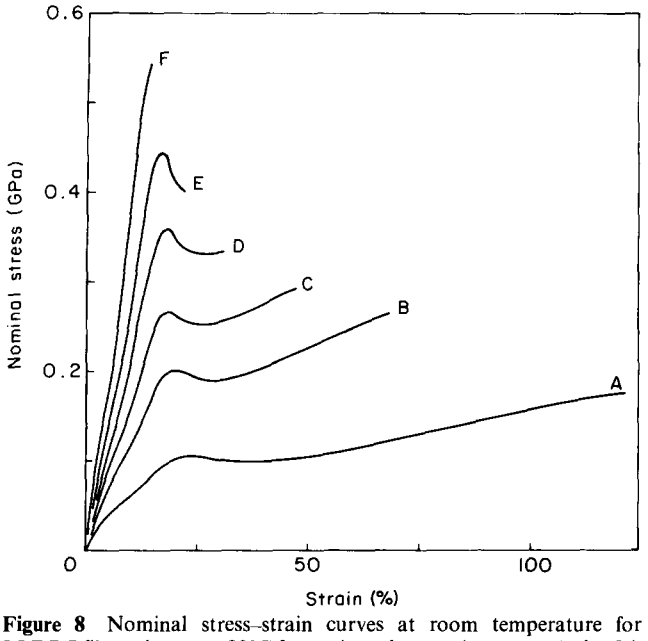

Figure 8 Nominal stress–strain curves at room temperature for LLDPE fibres drawn at 80°C for various draw ratios: curve A, $\lambda = 5.1$, $\sigma_r = 0.31$ GPa; B, $\lambda = 6.8$, $\sigma_r = 0.34$ GPa; C, $\lambda = 7.8$, $\sigma_r = 0.35$ GPa; D, $\lambda = 8.7$, $\sigma_r = 0.38$ GPa; E, $\lambda = 9.7$, $\sigma_r = 0.43$ GPa; F, $\lambda = 10.9$, $\sigma_r = 0.54$ GPa (σ_r is the actual tensile stress at break with respect to the fibre cross section after rupture)

effects (e.g. crystal continuity in the drawing direction, transverse crystalline block size, fibril length, densities of chain entanglements and intercrystalline tie chains, etc.).

In another connection, the increase in the magnitude of the tensile modulus with draw ratio cannot be accounted for by the increase in crystallinity and chain orientation, in the same range of strain (see *Figures 1* and *6*). Accordingly, and considering Peterlin's model for drawn fibres[26], we may suspect that the number of intercrystalline tie molecules partly or fully relaxed could be a factor of major importance as regards the stiffness of the LLDPE fibres. Further work is in progress to test this hypothesis.

Stress–elongation curves of LLDPE fibres recorded at room temperature are displayed in *Figure 8*, for different values of the fibre draw ratio. Also indicated is the actual strength at break of the fibres, calculated with respect to the fibre cross section after rupture. The curves of *Figure 8* exhibit a yield and a subsequent cold drawing that decreases with increasing draw ratio, at the same time as an improvement in stiffness and strength. No residual plastic deformation is observed for the fibre having the highest draw ratio.

The rise in tensile strength with draw ratio can be related to the ease with which the chains unfold during hot drawing, which helps to establish a good deal of intercrystalline tie molecules with reduced chain scissioning. It is clear that the cold drawing of a partially hot-drawn fibre is not as efficient as hot drawing in generating intercrystalline tie molecules capable of sharing the load. Thus, the greater the draw ratio produced by the hot drawing, the better the load distribution inside the fibre during the subsequent cold drawing, and the higher the strength at break.

CONCLUSIONS

During the course of tensile drawing, LLDPE undergoes structural changes that improve crystalline organization (increase in crystallinity, narrowing of crystal size distribution and slight thickening of crystals). The strain-induced crystallization of amorphous chains that leads to optimum crystallinity seems to promote the forced inclusion of some comonomer units within the crystal lattice.

The variation of the tensile modulus of the LLDPE fibres increases drastically with draw ratio, but the limiting value remains about 10 times lower than for HDPE fibres because of a much reduced drawability. It is suggested that the number of intercrystalline tie molecules might have a more important effect than chain tautness as regards the LLDPE fibre stiffness.

Tensile strength also increases with draw ratio, highlighting the fact that hot drawing makes chain unfolding easier and facilitates the creation of intercrystalline tie molecules that improve the load distribution within the fibres.

ACKNOWLEDGEMENTS

The authors wish to thank the Société Chimique des Charbonnages de France and the Agence Française pour la Maîtrise de l'Energie for a grant to support this work. The technical assistance of M. Rossignol in the tensile modulus measurements is gratefully acknowledged.

REFERENCES

1 Capaccio, G. and Ward, I. M. *J. Polym. Sci., Polym. Phys. Edn.* 1984, **22**, 475
2 Séguéla, R. and Rietsch, F. *Eur. Polym. J.* 1984, **20**, 765
3 Benelhadjsaid, C. and Porter, R. S. *J. Appl. Polym. Sci.* 1985, **30**, 741
4 Richardson, M. J., Flory, P. J. and Jackson, J. B. *Polymer* 1963, **4**, 221
5 Davis, G. T., Eby, R. K. and Martin, G. M. *J. Appl. Phys.* 1968, **39**, 4973
6 Wunderlich, B. 'Macromolecular Physics', Vol. 1: 'Crystal Structure, Morphology and Defects', Academic Press, New York, 1973, Ch. III
7 Sanchez, I. C. and Eby, R. K. *J. Res. Natl. Bur. Stand.* 1973, **77A**, 353
8 Wilchinsky, Z. W. *J. Polym. Sci., Polym. Phys. Edn.* 1968, **6**, 281
9 Baltà-Calleja, F. J., Gonzàlez Ortega, J. C. and Martinez de Salazar, J. *Polymer* 1978, **19**, 1094; Martinez de Salazar, J. and Baltà-Calleja, F. J. *J. Cryst. Growth* 1980, **48**, 283
10 Volkenstein, M. V. 'Configurational Statistics of Polymeric Chains', Wiley–Interscience, New York, 1963, Ch. 7
11 Mead, W. T., Desper, C. R. and Porter, R. S. *J. Polym. Sci., Polym. Phys. Edn.* 1979, **17**, 859
12 Pietralla, M., Grossman, H. P. and Krüger, J. K. *J. Polym. Sci., Polym. Phys. Edn.* 1982, **20**, 1193
13 Meinel, G. and Peterlin, A. *J. Polym. Sci., Polym. Phys. Edn.* 1971, **9**, 67
14 Glenz, W. and Peterlin, A. *J. Macromol. Sci. Phys.* 1970, **B4**, 473
15 Capaccio, G. and Ward, I. M. *Polymer* 1974, **15**, 233
16 Cacković, H., Loboda-Cacković, J. and Hosemann, R. *J. Polym. Sci., Polym. Symp. Edn.* 1977, **58**, 59
17 Baltà-Calleja, F. J. and Hoseman, R. *J. Polym. Sci., Polym. Phys. Edn.* 1980, **18**, 1159
18 Glenz, W., Morosoff, N. and Peterlin, A. *J. Polym. Sci., Polym. Lett. Edn.* 1971, **9**, 211
19 Hoshino, S., Powers, J., Legrand, D. G., Kawai, H. and Stein, R. S. *J. Polym. Sci.* 1962, **58**, 185
20 Samuels, R. J. 'Structured Polymer Properties', Wiley–Interscience, New York, 1974, p. 61
21 Kyu, T., Yamada, M., Shuehiro, S. and Kawai, H. *Polym. J.* 1980, **12**, 809
22 Cembrola, R. J., Kyu, T., Shuehiro, S., Kawai, H. and Stein, R. S. *J. Polym. Sci., Polym. Phys. Edn.* 1982, **20**, 1279
23 Capaccio, G., Crompton, T. A. and Ward, I. M. *J. Polym. Sci., Polym. Phys. Edn.* 1976, **14**, 1641; 1980, **18**, 301
24 Barham, P. J. and Keller, A. J. *J. Mater. Sci.* 1976, **11**, 27
25 Jarecki, L. and Meier, D. J. *Polymer* 1979, **20**, 1078
26 Peterlin, A. in 'Ultra-High Modulus Polymers' (Eds. A. Ciferri and I. M. Ward), Applied Science, London, 1979, Ch. 10